

Solar energetic particle anisotropies from the ace solar isotope spectrometer

R. A. Leske¹, G. A. de Nolfo², C. M. S. Cohen¹, E. R. Christian², A. C. Cummings¹, R. A. Mewaldt¹, P. L. Slocum³, E. C. Stone¹, T. T. von Rosenvinge², and M. E. Wiedenbeck³

¹California Institute of Technology, Pasadena, CA 91125 USA

²NASA/Goddard Space Flight Center, Code 661, Greenbelt, MD 20771 USA

³Jet Propulsion Laboratory, Pasadena, CA 91109 USA

Abstract. Although not specifically designed for it, the Solar Isotope Spectrometer (SIS) on the Advanced Composition Explorer spacecraft is sensitive to particle anisotropies of heavy ions at energies of tens of MeV/nucleon. Using the arrival time of each particle (to the nearest second) and the trajectory measured with the instrument's position sensing detector, the arrival direction of each particle may be determined to $\sim 30^\circ$ in azimuth about the spacecraft spin axis and to better than 1° in zenith angle from the axis. This allows the angular distribution of particles to be measured within the $\sim 145^\circ$ wide field of view of the instrument, from which the intensities both along the field and perpendicular to it can usually be determined. We describe how anisotropies are obtained from SIS and present examples demonstrating some of the capabilities of SIS in studying anisotropies. With further analysis, SIS can contribute to studies exploring the dependence of particle angular distributions on energy and species.

telescopes either mounted at different angles to the spin axis of spacecraft such as ISEE 3 (Sanderson et al., 1985), Wind (Reames et al., 2001) or ACE (Hawkins III et al., 2000) or mounted on a three axis stabilized spacecraft such as Voyager (Cummings and Stone, 1999), and even 3-D measurements using a single telescope equipped with trajectory-sensing capabilities with a wide field of view on a three axis stabilized spacecraft such as SOHO (Torsti et al., 2000).

We have recently come to appreciate the fact that the Solar Isotope Spectrometer (SIS) on the Advanced Composition Explorer (ACE) spacecraft can also be used to examine anisotropies, particularly anisotropies of heavy ions at energies of tens of MeV/nucleon. In this report, we will describe the approach used to obtain anisotropy information from SIS data, discuss the advantages and limitations of doing so, and qualitatively illustrate the capabilities of the instrument with a few examples. Significantly more analysis is required to obtain quantitative results, and this is very much a work in progress.

1 Introduction

Measurements of particle pitch angle distributions and anisotropies provide an important tool to study the interplanetary acceleration and transport of many types of energetic particles. Recent studies, for example, have used differences between particle anisotropies and the magnetic field direction to measure the ratio of perpendicular to parallel diffusion coefficients in corotating interaction regions (Dwyer et al., 1997), and temporal variations of anisotropies have been used to examine the isotropization of solar energetic particles (SEPs) by proton-generated Alfvén waves (Reames et al., 2001).

A wide variety of techniques using different types of instruments and observing platforms have been employed for measuring anisotropies. A few examples include measurements of two-dimensional angular distributions from a spinning spacecraft such as Pioneer 6 (e.g., Fan et al. (1966)), three dimensional anisotropy measurements using several

2 Technique

The SIS instrument is primarily designed to measure the nuclear charge, Z , mass, M , and energy spectra for elements from He to Ni at energies of ~ 3 to ~ 200 MeV/nucleon using the dE/dx versus residual energy technique in a pair of silicon solid-state detector telescopes (Stone et al., 1998b). Unlike many instruments used specifically to study anisotropies, SIS does not measure sector count rates. Most of the rates measured by SIS are accumulated over 256 s, with up to 18 "high resolution" rates read out every 32 s, but even these are essentially useless for anisotropy studies when measured on a spacecraft with a ~ 12 s spin period (Stone et al., 1998a). However, the principle type of science data returned by SIS is pulse height analyzed (PHA) events rather than rates, and these are time tagged to the nearest second by the telemetry minor frame in which they are sent to the ground. Also, each such PHA event includes trajectory information measured by

SIS with a pair of two dimensional position sensitive strip detectors (Stone et al., 1998b), from which the path of each particle relative to the instrument can be reconstructed with an accuracy of $\sim 1^\circ$.

SIS is mounted on the top (sunward-facing) deck of ACE with its boresight tilted 25° from the normal to the deck. The spacecraft rotates about this normal, and SIS has a 95° full angle field of view, so during each rotation SIS is able to view particles within a 145° -wide cone centered on the spin axis. During ACE's halo orbit about the L1 Lagrange point, the spin axis is pointed to within $\sim 5^\circ$ to 10° of the Sun essentially at all times (Stone et al., 1998a). Thus, for example, when the interplanetary magnetic field direction is at its nominal angle of $\sim 45^\circ$ from the spacecraft-to-Sun line, the field direction is at least 17.5° (and often as much as 37.5°) inside the edge of the spin-averaged field of view of SIS. Even during moderately disturbed field conditions, both the direction along the field line and perpendicular to it are visible. With a field of view of $< 180^\circ$, SIS can not directly observe bi-directional streaming of particles (unless the pitch angle distributions are sufficiently broad; see discussion below). During the relatively rare occasions when the field direction is nearly perpendicular to the spacecraft spin axis, both directions along the field are outside SIS's field of view.

The angular distributions shown in this paper are obtained from SIS PHA events that have been selected by element or energy interval. Certain standard quality criteria, such as consistency between multiple determinations of Z , were also imposed, and trajectories were required to be consistent with particles stopping in the instrument. Trajectory information gives the arrival direction of each selected particle relative to the instrument to within $\sim 1^\circ$, and a series of coordinate rotations transforms this to a trajectory relative to the spinning spacecraft coordinate system. Sun sensors on ACE generate a sunpulse every rotation, and the sunpulse times are each recorded to the nearest millisecond and telemetered for use in ground analysis. The time difference between the minor frame containing each selected event and the nearest previous sunpulse time relative to the time between successive sunpulses gives the clock angle of the spacecraft (measured from the sunpulse line) at the time of the event with a 1 s timing accuracy, or $\sim 30^\circ$ angular accuracy, which allows the particle trajectories to be transformed to a non-rotating frame in spacecraft coordinates.

The distributions are calculated relative to the magnetic field direction provided by the magnetometer (MAG) instrument on ACE. Magnetic field components from calibrated and verified "Level 2" data, measured every 16 s, are interpolated to the detection time of each particle and converted to despun spacecraft coordinates by using spacecraft attitude information. The direction of every recorded particle can then be compared to the interpolated direction of the B field at that time, and distributions can be made of the differences. Although angular resolution in the "zenith" direction (angle from the spin axis) is better than in the "azimuthal" direction (angle about the spin axis) since it does not depend on the limited timing accuracy, the particle detection efficiency

is a strong function of the zenith-angle-dependent geometry factor. Corrections for this effect are necessary on an event-by-event basis when comparing with the time-varying zenith angle of the B-field and are only in an early stage of development, so zenith angle distributions will not be discussed here but can be obtained with further analysis.

Although the azimuthal resolution for a single particle is only $\sim 30^\circ$, the centroid of a collection of particles can, of course, be determined to much greater accuracy. The fact that the spin period is not exactly 12 s and therefore generally not commensurate with the 1 s readout interval also helps to improve the resolution when summing over multiple rotations. Because of a finite delay between the arrival of a particle in the detector, the processing of the pulse heights for that particle by SIS, and the time-tagging of the event when the telemetry frame is assembled by ACE, the azimuthal direction of the B-field lags that of the particle anisotropy derived from the event timing. Empirically we find that the average difference is $\sim 50^\circ$, and we have subtracted this angle from the azimuthal direction of each particle. We have not converted from the spacecraft reference frame to the frame co-moving with the solar wind to eliminate the Compton-Getting effect, which should be small for these particles with velocities ~ 60 – 200 times that of the solar wind.

3 Discussion

We have binned all the good SIS PHA events for the mission to date into time bins of varying length but each containing the same number of particles (typically 300), and we have examined the distribution of the difference between the azimuthal component of the particle arrival direction and that of the B-field in each bin. We find anisotropies to be fairly common at these energies, and they often occur at the onset of SEP events. This survey with SIS has found significant anisotropies in nearly all the SEP anisotropy periods discussed by Reames et al. (2001) at lower energies, including the November 1997 period which was also studied at energies similar to SIS by SOHO (Torsti et al., 2000).

Examples of anisotropies observed by SIS are illustrated in Figs. 1 and 2. The gradual SEP event of 4 April 2000 is shown in Fig. 1. This event was associated with a C9.7/2F X-ray flare from N16W66, and the impact of the associated shock with $B_z \sim -25$ nT on the magnetosphere triggered a major geomagnetic storm in which the geomagnetic activity index Dst reached -321 nT. This event featured both large anisotropies and high count rates, allowing us to examine how the anisotropy depends on energy and species.

Significant anisotropies are seen in SIS through most of the period from day 95.7 to 97.7, with qualitatively similar features appearing in the angular distributions of 3.4–6.1 MeV/nucleon He, 6.1–13.6 MeV/nucleon He, and 7–30 MeV/nucleon O as shown. (Although the He fluxes are higher than those of O, as shown in the top panel, SIS only processes a small sample of the He PHA events so the bin sizes needed to maintain the same statistical accuracy in the

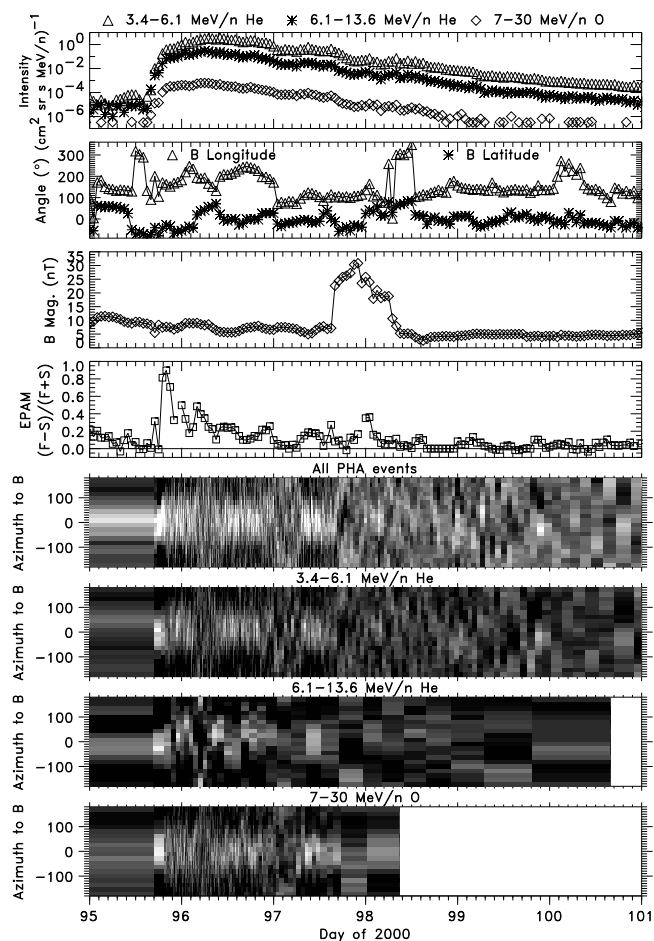


Fig. 1. Measured quantities from ACE during 4–10 April 2000 plotted versus time. The first 4 panels show hourly-averaged ACE Level 2 data available from <http://www.srl.caltech.edu/ACE/ASC/level2>. Top panel: intensities from SIS for 3.4–6.1 MeV/n He (triangles), 6.1–13.6 MeV/n He (asterisks), and 7–30 MeV/n O (diamonds). Second panel: magnetic longitude (triangles) and latitude (asterisks), both in RTN coordinates, from ACE/MAG. Third panel: B-field magnitude from ACE/MAG. Fourth panel: coarse anisotropy indicator from ACE/EPAM, comparing intensities of 1.9–4.75 MeV ions (mostly protons) toward the front (“F”, from the LEMS30 sensor (Gold et al., 1998)) and side (“S”, from LEMS120 (Gold et al., 1998)); the calculated ratio $(F-S)/(F+S)$ is shown. Fifth panel: Distribution of the difference between the azimuthal angle (about the spacecraft spin axis) of each good PHA event detected by SIS and that of the B-field direction at the same time (interpolated from 16 s averaged ACE/MAG data), with 300 events in each time bin subdivided into 20 equal angle bins. Sixth panel: Same as fifth panel, but using only 3.4–6.1 MeV/n He PHA events. Seventh panel: Same as fifth panel, but using only 6.1–13.6 MeV/n He PHA events, with 200 counts in each time bin. Eighth panel: Same as fifth panel, but using only 7–30 MeV/n O PHA events, with 200 counts in each time bin. The absolute number of counts for each grey-scale shade varies among the bottom 4 panels, but in each case runs from black at low intensity to white at high, with a dynamic range of about a factor of 2 between the minimum and maximum displayed intensity.

anisotropy calculations are larger for He than for O in the bottom 2 panels.) The duration of this anisotropy is longer than

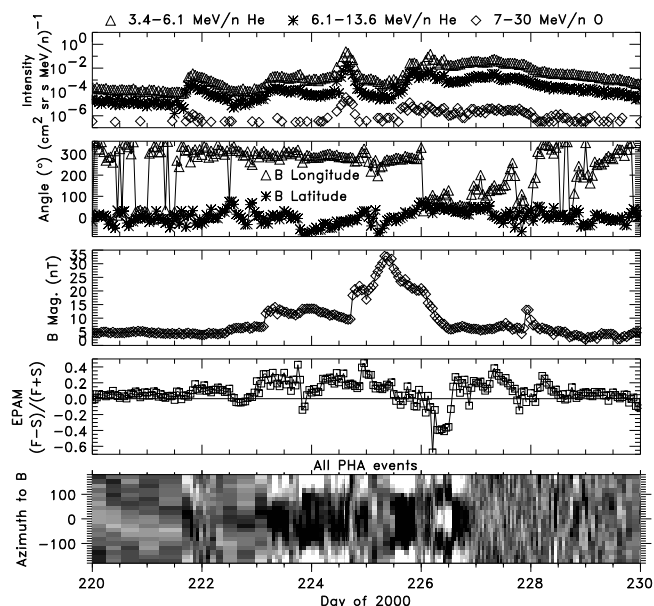


Fig. 2. Same as the top 5 panels of Fig. 1, only covering the period 7–17 August 2000.

most we observe, which often disappear after a few hours. There are noticeable dropouts or decreases in anisotropy centered around day 96.25 and 97.15. Large changes in the direction of the B-field might create such dropouts by moving the anisotropy direction out of the field of view of SIS, but while some direction changes are seen, the fact that strong anisotropies are present from 97.3 to 97.7 when the RTN B longitude is even less than in the first dropout suggests such directional changes probably are not responsible. A change in the B-field polarity would switch the anisotropy direction from 0° to $\pm 180^\circ$, which might be consistent with the observed anisotropy during the second dropout, but such a polarity change did not occur.

For comparison, we also show in Fig. 1 a crude indication of the anisotropy observed by the Electron, Proton, and Alpha Monitor (EPAM) on ACE (Gold et al., 1998). The quantity we show is a comparison of 1.9–4.75 MeV ions (mostly protons) measured by two Low Energy Magnetic Spectrometer (LEMS) subcomponents of EPAM, one oriented at 30° to the spin axis (LEMS30), and the other at 120° (LEMS120). This corresponds to look directions very roughly along and perpendicular to the nominal B-field direction. It should be noted that EPAM is capable of far more detailed and quantitative anisotropy measurements (see, e.g. Hawkins III et al. (2000)), but the quantity we show here is easily derived from publicly-available ACE Level 2 data and is sufficient to indicate interesting time periods. As shown in the figure, significant anisotropies are also seen by EPAM from day 95.7 to 97.7, including the dropout from 97.0 to 97.3. Most striking is the strong anisotropy spike at the onset of the SEP event, which is also clearly observed by SIS for all species shown.

A second example of SIS anisotropy measurements is shown in Fig. 2. Here particle fluxes were much lower, but

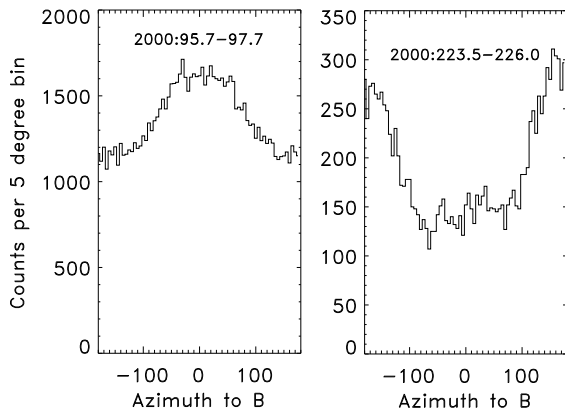


Fig. 3. Distribution of the difference between the azimuthal angle (about the spacecraft spin axis) of each good PHA event detected by SIS and that of the B-field direction at the same time (interpolated from 16 s averaged ACE/MAG data), summed over the indicated time periods.

showed rather complicated intensity variations. Solar activity included two M-class X-ray flares, one near the middle of day 221, the other in the middle of day 225. At least two CMEs passed ACE, one early on day 223 and the other late on day 224. A strong shock late on day 224, with B_z around -34 nT, triggered a geomagnetic storm with Dst down to -237 nT.

Since the particle rates are so much lower in Fig. 2, we have not subdivided the SIS PHA events by element and energy, but rather show just the anisotropy using all detected particles. Since the polarity of the B-field has changed compared to Fig. 1, particles arriving from the sunward field direction now appear at $\pm 180^\circ$ to the field. The anisotropies seen by SIS are much stronger in this period than in Fig. 1 and last for most of 4 consecutive days from day 223.0 to 227.0. (Note also the brief but clear anisotropy at the onset of the small SEP event late on day 221, which is more typical of the anisotropies seen by SIS.) Even more unusual for SIS, however, is the very clear indication of bi-directional streaming in the middle of day 226, when strong peaks are simultaneously observed at both 0° and $\pm 180^\circ$. At this time the B-field is approximately perpendicular to the spin axis, or $\sim 20^\circ$ beyond the field of view of SIS. However, since the particle pitch angle distributions are much broader than 20° , the large-angle tails of the distributions of particles coming from both directions along the field can be seen. Again, some indications of anisotropy are seen by EPAM during the same time periods as SIS, with a remarkable excess of particles from LEMS120 compared with LEMS30 precisely at the time bi-directional streaming is seen by SIS.

A somewhat clearer indication of the statistical significance of the anisotropies in the two examples discussed above is given in Fig. 3, where angular distributions summed over the periods of interest are shown. The average ratio of the intensity along the azimuthal component of the field to that perpendicular to it is ~ 1.4 during the first time period and more than 2.4 during the second. The pitch angle dis-

tribution appears to be substantially narrower in the second period, but this may indicate that only the tails of the distribution are being viewed and the peak is being missed.

Although the analysis is presently at a very early stage of development, we have demonstrated that SIS is certainly able to observe anisotropies which are correlated with the magnetic field direction and independently detected by other instruments. In spite of the limited angular field of view, measurements from SIS offer the possibility of studying anisotropies with good angular resolution across a broad range of species at energies higher than attainable by many other instruments.

Acknowledgements. We thank Andrew Davis for providing the sun-pulse timing data and for helpful discussions. We appreciate the work of the EPAM and MAG science teams in generating their Level 2 data products and that of the ACE Science Center in making these data readily available. Details on solar and interplanetary activity were obtained from NOAA through the Space Environment Center web site. This research was supported by NASA at the California Institute of Technology (under grant NAG5-6912), the Jet Propulsion Laboratory, and the Goddard Space Flight Center.

References

- Cummings, A. C. and Stone, E. C., Radial interplanetary mean free paths inferred from anomalous cosmic ray observations in the outer heliosphere, *Proc. 26th Internat. Cosmic Ray Conf. (Salt Lake City)*, 7, 496–499, 1999.
- Dwyer, J. R. et al., Perpendicular transport of low-energy corotating interaction region-associated nuclei, *Astrophys. J. Lett.*, 490, L115–L118, 1997.
- Fan, C. Y., Lampert, J. E., Simpson, J. A., and Smith, D. R., Anisotropy and fluctuations of solar proton fluxes of energies 0.6–100 MeV measured on the Pioneer 6 space probe, *J. Geophys. Res.*, 71, 3289–3296, 1966.
- Gold, R. E. et al., Electron, Proton, and Alpha Monitor on the Advanced Composition Explorer spacecraft, *Space Sci. Rev.*, 86, 541–562, 1998.
- Hawkins III, S. E., Roelof, E. C., Gold, R. E., Haggerty, D. K., and Ho, G. C., A survey of 40–300 keV electron events with beam-like anisotropies, in *Acceleration and Transport of Energetic Particles Observed in the Heliosphere: ACE 2000 Symposium*, edited by R. A. Mewaldt et al., no. 528 in AIP Conf. Proc., pp. 95–98, AIP, New York, 2000.
- Reames, D. V., Ng, C. K., and Berdichevsky, D., Angular distributions of solar energetic particles, *Astrophys. J.*, 550, 1064–1074, 2001.
- Sanderson, T. R., Reinhard, R., van Nes, P., and Wenzel, K.-P., Observations of three-dimensional anisotropies of 35- to 1000-keV protons associated with interplanetary shocks, *J. Geophys. Res.*, 90, 19–27, 1985.
- Stone, E. C. et al., The Advanced Composition Explorer, *Space Sci. Rev.*, 86, 1–22, 1998a.
- Stone, E. C. et al., The Solar Isotope Spectrometer for the Advanced Composition Explorer, *Space Sci. Rev.*, 86, 357–408, 1998b.
- Torsti, J., Mäkelä, P., Teittinen, M., and Laivola, J., SOHO/Energetic and Relativistic Nucleon and Electron experiment measurements of energetic H, He, O, and Fe fluxes during the 1997 November 6 solar event, *Astrophys. J.*, 544, 1169–1180, 2000.